DOI: 10.15669/pnst.7.199

Progress in Nuclear Science and Technology
Volume 7 (2025) pp. 199-206

ARTICLE

Chromatographic separation properties of metal ions from simulated high-level liquid waste using sulfur-containing amic acid-functionalized silica gel

Naoki Osawa [a, b], Tatsuya Ito [c], Taiga Kawamura [a], Hao Wu [d] and Seong-Yun Kim [a, *]

[a] *Department of Quantum Science and Energy Engineering, Graduate School of Engineering, Tohoku University, Sendai, Miyagi 980-8579, Japan;* [b] *Japan Nuclear Fuel Limitted, Rokkasho, Kamikita, Aomori 039-3212, Japan;* [c] *Japan Atomic Energy Agency, Tokai, Naka, Ibaraki 319-1195, Japan;* [d] *School of Nuclear Science and Engineering, Shanghai Jiao Tong University, Shanghai, China*

Technologies for separating and recovering elements contained in high-level liquid waste (HLLW) generated at reprocessing plants can contribute to reducing the volume of high-level radioactive waste while enabling resource recovery. This study synthesized three types of thiodiglycolamic acid-functionalized silica gels TDGAA-Si, TDGAA2-Si, and TDGAA3-Si, by adding thiodiglycolic anhydride to 3-aminopropyl-functionalized, 3-(ethylenediamino)propyl-functionalized, and 3-(diethylenetriamino)propyl-functionalized silica gels, respectively. Then, we conducted batch-adsorption and chromatographic separation experiments using simulated HLLW containing 15 metal ions based on adsorption selectivity, contact time, temperature, and separation properties. The three adsorbents showed good separation performances for Pd(II) from the investigations using thiourea as an eluent. In contrast, Ru(III) and Rh(III) were difficult to separate at 298 K, but their uptake ratios could be improved by raising their temperatures. Investigations also revealed that the separation of Zr(IV) resulted in slightly differing characteristics depending on the adsorbent used. For instance, TDGAA-Si showed high separation performance with Zr(IV) at 80 mm bed height and 298 K, whereas using TDGAA2-Si and TDGAA3-Si, most Zr(IV) tended to flow out just behind the feed solution. Beside, as a result of evaluating the adsorption properties of TDGAA3-Si depending on the bed height, we confirm that while Zr(IV) and Mo(VI) are most suitable for accumulation on the adsorbent, Re(VII) is suitable for separation via peak shifts by setting an appropriate bed height.

Keywords: chromatographic separation; adsorbent; functionalized silica gel; simulated high-level liquid waste

Nomenclature

C_0	Metal ion concentration at initial time (mM = mmol dm^{-3})	t	Experiment time (min)
C_e	Metal ion concentration at equilibrium state (mM)	t_{Ve}	Experiment time while certain effluent volume flows (min)
C_t	Metal ion concentration a certain time t (mM)	t_{Feed}	Maximum peak position of the non-adsorbed metal ion (min)
h	Bed height of the adsorbent (mm)	t_{metal}	Maximum peak position of the metal ion (min)
m	Weight of the adsorbent (g)	V	Volume of simulated HLLW (cm^3)
R_B	Uptake ratio in batch-adsorption experiment (%)	V_E	Effluent volume of chromatographic experiment (cm^3)
R_C	Uptake ratio in chromatographic experiment (%)	V_{Feed}	Volume of feed solution (cm^3)
R_u	Universal gas constant (kJ K^{-1} mol^{-1})	V_f	Fractionated volume of effluent (cm^3)
T	Temperature (K)	ΔH^0	Changes in enthalpy (kJ mol^{-1})
		ΔG^0	Changes in Gibbs free energy (kJ mol^{-1})
		ΔS^0	Changes in entropy (kJ mol^{-1} K^{-1})

1. Introduction

Since high-level liquid waste (HLLW) generated at reprocessing plants contains various nuclides with different properties, their complexity makes waste management and disposal difficult [1]. Therefore, technologies for separating and recovering elements contained in HLLW can contribute to reduction in the volume of high-level radioactive waste and promotion of resource recovery. As a nuclide separation method, research is being pursued on the solvent extraction method, precipitation method, extraction chromatography method, and others [2,3]. Among these methods, extraction chromatography has evident advantages, such as the need for only a small amount of organic solvent, ease of solid–liquid separation, and simple equipment configuration [4]. Furthermore, as an adsorbent

*Corresponding author. E-mail: sonyun.kimu.d7@tohoku.ac.jp

for extraction chromatography, macroporous silica polymer composite particles, which have preferred mechanical strength and radiation resistance, have also been used as a base material, where their pore is impregnated with an extractant to impart an adsorption function [5]. Based on the research on metal adsorption in solvent extraction, impregnated silica-based adsorbents with various adsorption capacities have been developed. Particularly, studies have confirmed that impregnated silica-based adsorbents with a thiodiglycolamide (TDGA) structure exhibit sufficient palladium adsorption performance [6-8]. However, there is concern regarding durability deterioration due to extractant leakage and organic layer formation [9,10]. To this end, the applicability of functionalized silica-based adsorbents as another approach was evaluated using thiodiglycolamic acid functionalized silica gel (TDGAA-Si) [9]. From the experimental results, the functionalized silica-based adsorbent exhibited element selectivity. Hence, their applications were considered in the recovery of metal ions from HLLW. Conversely, analytical research to predict extraction chromatography's adsorption and separation phenomena are indispensable for practical usage. Also, the different adsorption and elution behavior should be reproduced for each metal ion. Therefore, based on these facts, we evaluated the adsorption and separation behavior on a column as an adsorbent performance preliminary assessment using three types of thiodiglycolamic acid-functionalized silica gels: TDGAA-Si, TDGAA2-Si, and TDGAA3-Si, synthesized by adding thiodiglycolic anhydride to 3-aminopropyl-functionalized silica gel, 3-(ethylenediamino)propyl-functionalized silica gel, and 3-(diethylenetriamino)propyl-functionalized silica gel, respectively.

2. Experimental

2.1. Materials

Of the materials used for this study's investigation, we employed a nitric acid including each 5 mM of 15 metal ions (Ru, Rh, Pd, Zr, Mo, Re, Cs, Sr, Ba, La, Ce, Nd, Sm, Eu, and Gd) as the simulated HLLW. We then reproduced a simulated HLLW using a ruthenium nitrosyl nitrate solution, rhodium nitrate solution, palladium nitrate solution (Sigma-Aldrich Chemical Co. LLC, Saint Louis, Missouri, USA), nitrates ($ZrO(NO_3)_2{\cdot}2H_2O$, $CsNO_3$, $Sr(NO_3)_2$, $Ba(NO_3)_2$, and $RE(NO_3)_3{\cdot}6H_2O$ (RE = La, Ce, Nd, Sm, Eu, and Gd), Kanto Chemical Co. Inc., Tokyo, Japan), molybdate ($(NH_4)_6Mo_7O_{24}{\cdot}4H_2O$, Kanto Chemical Co. Inc.), oxide (Re_2O_7, Mitsuwa Chemicals Co. Ltd., Osaka, Japan), deionized water, and concentrated nitric acid. Since the number and concentration of metal ions of the actual HLLW were quite complicated, we used the 15 representative metal ions at a constant concentration to evaluate the adsorption and separation performance of the adsorbent.

Notably, while 3-aminopropyl-functionalized silica gel (Amino-Si, loading amount: 1.0 mmol g^{-1}), 3-(ethylenediamino)propyl-functionalized silica gel (Ethylenediamino-Si, loading amount: 1.4 mmol g^{-1}), and 3-(diethylenetriamino)propyl-functionalized silica gel (Dietylenetriamino-Si, loading amount: 1.3 mmol g^{-1}) were the base materials, thiodiglycolic anhydride (purity: 95 %) was the function-imparting material of the sulfur-containing amic acid-functionalized silica gel, respectively. Herein, Amino-Si, Etylenediammino-Si, and Diethylenetriamino-Si were procured from Sigma-Aldrich Chemical Co. LLC, whereas thiodiglycolic anhydride was from Toronto Research Chemicals Inc. (Toronto, Ontario, Canada).

2.2. Preparation of functionalized adsorbents

Figure 1 shows the preparation procedure of a sulfur-containing amic acid-functionalized silica gel. Notably, the synthesis was carried out following studies using diglycolamic anhydride and thiodiglycolamic anhydride [9,11]. The base material and thiodiglycolic anhydride amounts at synthesis were 50.0 g (Amino-Si) and 8.2 g (thiodiglycolic anhydride) for TDGAA-Si, 20.0 g (Ethylenediamino-Si) and 9.2 g for TDGAA2-Si, and 20.0 g (Diethylenetriamino-Si) and 12.8 g for TDGAA3-Si, respectively. First, we washed Amino-Si, Ethylemediamino-Si, and Diethylenetriamino-Si with methanol to remove impurities. Mixtures of each silica gel, thiodiglycolic anhydride, and dichloromethane were then stirred for three days at room temperature using a shaker. After the reaction, we sequentially washed the synthetic materials with dichloromethane, deionized water, and methanol and vacuum-dried them at 313 K. The total TDGAA-Si, TDGAA2-Si, and TDGAA3-Si amounts in the present synthesis were 55.3, 24.0, and 23.9 g, respectively. **Figure 2** shows the thermogravimetric analysis results of TDGAA2-Si and

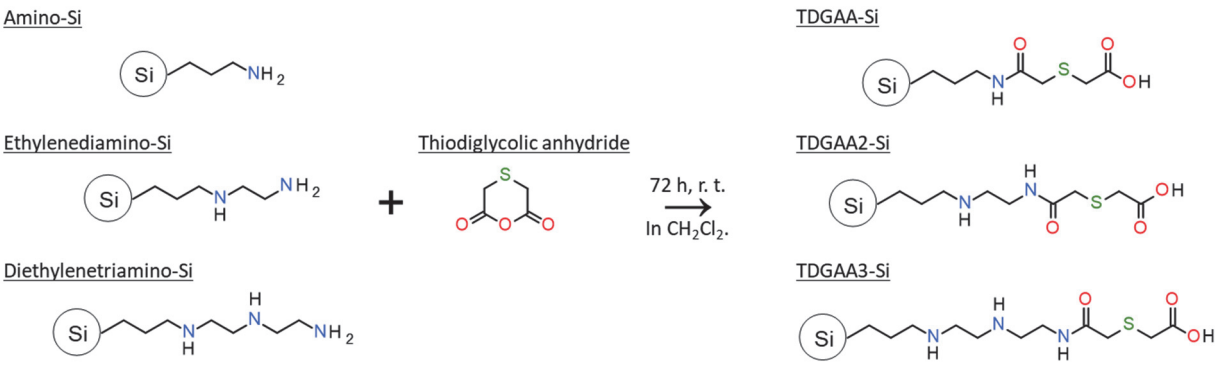

Figure 1. Preparation of TDGAA-Si, TDGAA2-Si, and TDGAA3-Si.

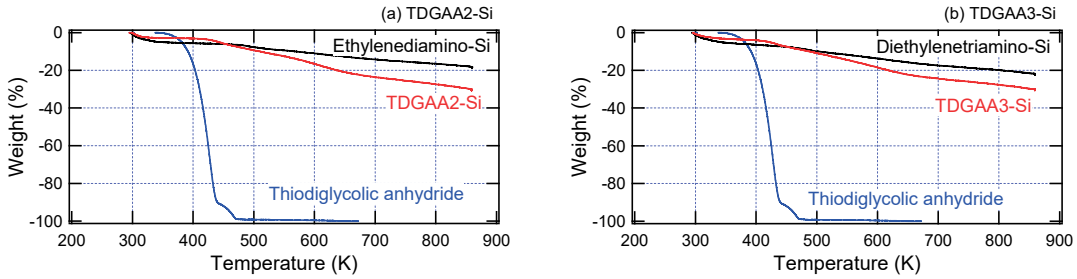

Figure 2. Thermal gravimetric curves for (a) TDGAA2-Si and (b) TDGAA3-Si.

TDGAA3-Si. While the weight reduction of TDGAA2-Si and TDGAA3-Si appeared around 300 K and became noticeable after about 400 K under N_2 conditions, calculating the reaction ratio of thiodiglycolic anhydride to Ethylemediamino-Si and Diethylenetriamino-Si based on the weight ratio gave 87% and 66%, respectively.

2.3. Batch-adsorption experiments

Subsequently, we evaluated the adsorption selectivity, contact time dependence, and temperature dependence of metal ion adsorption using TDGAA2-Si and TDGAA3-Si via batch-adsorption experiments. These experiments were conducted under 2 M HNO_3 conditions, a varying contact time of 10 min to 24 h, and a temperature of 288 to 323 K. The experimental procedure was as follows: First, 0.2 g of the adsorbent and 4 cm^3 of the simulated HLLW were put into a glass vial at a solid–liquid ratio of 20. Then, the adsorbent and simulated HLLW mixture was shaken at 160 rpm using a water bath shaker, after which the solid and liquid phases were separated using a regenerated cellulose membrane filter with a 0.45 µm pore size. Finally, we evaluated the adsorption performance of the adsorbent by measuring the concentration of the metal ions remaining in the liquid phase using an atomic absorption spectrometer for Cs(I) and an inductively coupled plasma atomic emission spectrometer for the other 14 metal ions.

2.4. Chromatographic separation experiment

This study also evaluated the adsorption and separation properties using column chromatography to continuously recover multiple nuclides in simulated HLLW. We conducted two types of experiments: evaluation of the three adsorbents (TDGAA-Si, TDGAA2-Si, and TDGAA3-Si) and evaluation of the effect of adsorbent bed height on adsorption performance. While the amount of adsorbent packed into the column was 80 mm in the first experiment, it was 80, 160, and 240 mm in the second experiment. First, thermo-stated water was supplied to the outer jacket of the glass column to keep the temperature constant at 298 or 323 K. Then, 5 cm^3 of simulated HLLW containing 15 metal ions at 5 mM as the feed solution, 50 cm^3 of 2 M HNO_3 as the washing solution, 30 cm^3 of 0.1 M thiourea in 0.01 M HNO_3 solution as the first eluent, and 0.01 M diethylenetriamine pentaacetate acid (DTPA) as the second eluent were sequentially put into a column packed with an adsorbent at a flow rate of 0.3 cm^3 min^{-1}. The collected solution that passed through the column was also fractionated every 3 cm^3. Finally, we measured the metal ion concentration in the solution using an atomic absorption spectrometer and an inductively coupled plasma atomic emission spectrometer like the batch-adsorption experiments.

3. Results and Discussion

3.1. Adsorption selectivity

The adsorption selectivities of TDGAA2-Si and TDGAA3-Si using simulated HLLW containing 5 mM of the 15 metal ions under 2 M HNO_3 and a 5 h contact time at 297 and 323 K are shown in **Figure 3**. The uptake ratio R_B (%) of the metal ion shown in Figure 3 is described as follows:

$$R_B = \frac{C_0 - C_t}{C_0} \times 100. \quad (1)$$

Investigations revealed that the adsorption selectivities of TDGAA2-Si and TDGAA3-Si showed similar trends due to the thiodiglycolic acid, which contributes greatly to adsorption. Specifically, while the uptake ratio of Pd(II) on both adsorbents was above 90%, it was also well adsorbed

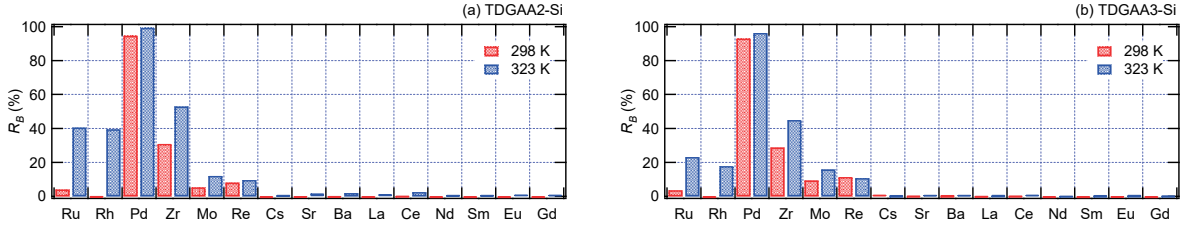

Figure 3. Adsorption selectivity of (a) TDGAA2-Si and (b) TDGAA3-Si. [Metal]: 5 mM for the 15 metal ions, [HNO_3]: 2 M, temperature: from 298 K to 323 K, contact time: 5 h.

at 298 and 323 K. This high adsorption performance toward Pd(II) was due to the high affinity between the soft donor (sulfur of thiodiglycolic acid) and soft metal (palladium) based on the hard and soft (Lewis) acids and bases theory [12]. In contrast, although Ru(III) and Rh(III) were not well adsorbed on TDGAA2-Si and TDGAA3-Si, their adsorption performances improved with increasing temperature. Adsorption of Cs (alkali metals), Sr, Ba (alkaline earth metals), La, Ce, Nd, Sm, Eu, and Gd (rare earth elements) could be hardly observed.

3.2. Effect of contact time

Subsequently, we evaluated the adsorption kinetics when TDGAA2-Si and TDGAA3-Si were used via batch-adsorption experiments, with time varying from 10 min to 24 h in the presence of 2 M HNO_3 at 298 K. The uptake adsorption ratios of the 15 metal ions are shown in **Figure 4**. Investigations revealed that Pd(II) adsorption reached equilibrium within about 10 h for both TDGGAA2-Si and TDGAA3-Si. Since in a previous study, TDGAA-Si reached the adsorption equilibrium quickly [9], we propose that Pd(II) adsorption on these adsorbents was relatively slow. Focusing on other metal ions, the adsorption of Zr(IV) onto TDGAA2-Si was above 50% at 24 h, which is equivalent to that of TDGAA-Si [9]. As for Ru(III) and Rh(III) when TDGAA-Si was used, while the adsorption amount was about 35% at 24 h [9], adsorption decreased in TDGAA2-Si and TDGAA3-Si. Although the adsorption selectivity results showed that the adsorption of Ru(III) and Rh(III) were enhanced by increasing temperature, the reaction was very slow at 298 K, proposing its ineffectiveness in increasing the adsorption amount over time.

3.3. Effect of temperature

Figure 5 shows the van 't Hoff plot, which describes the relationship between $\ln(K_d)$ and T^{-1}, to explain the effects of reaction temperature on the adsorption of Ru(III), Rh(III), Pd(II), Zr(IV), Mo(VI), and Re(VII) within the range of 288–323 K. **Table 1** summarizes the thermodynamic parameters for the adsorption of six metal ions onto TDGAA2-Si and TDGAA3-Si. The expressions for the metal ion's distribution coefficient, the van 't Hoff equation, and the Gibbs free energy equation are described as follows [13,14]:

$$K_d = \frac{C_0 - C_e}{C_e} \times \frac{V}{m}, \quad (2)$$

$$ln\, K_d = -\frac{\Delta H^0}{R_u T} + \frac{\Delta S^0}{R_u}, \quad (3)$$

$$\Delta G^0 = \Delta H^0 - \Delta S^0 T. \quad (4)$$

The positive values for ΔH^0, except for Re(VII) on

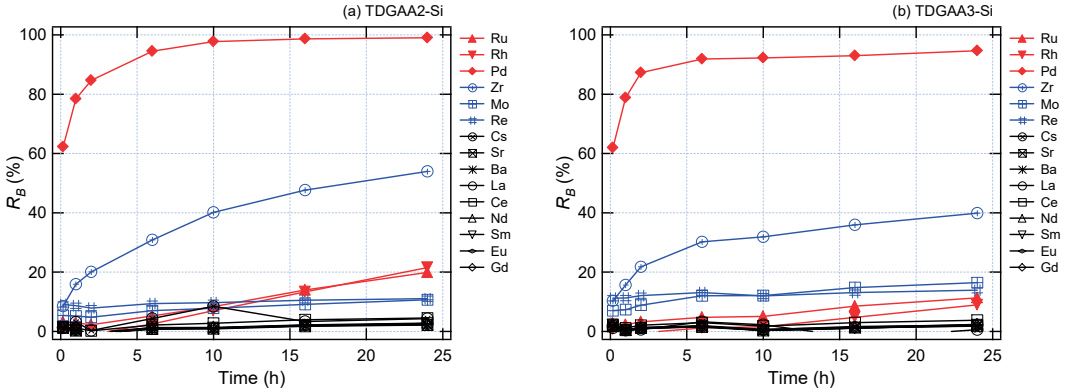

Figure 4. Relationship between the uptake ratio of the 15 metal ions and their contact times by (a) TDGAA2-Si and (b) TDGAA3-Si. [Metal]: 5 mM for 15 metal ions, [HNO_3]: 2 M, temperature: 298 K, contact time: from 10 min. to 24 h.

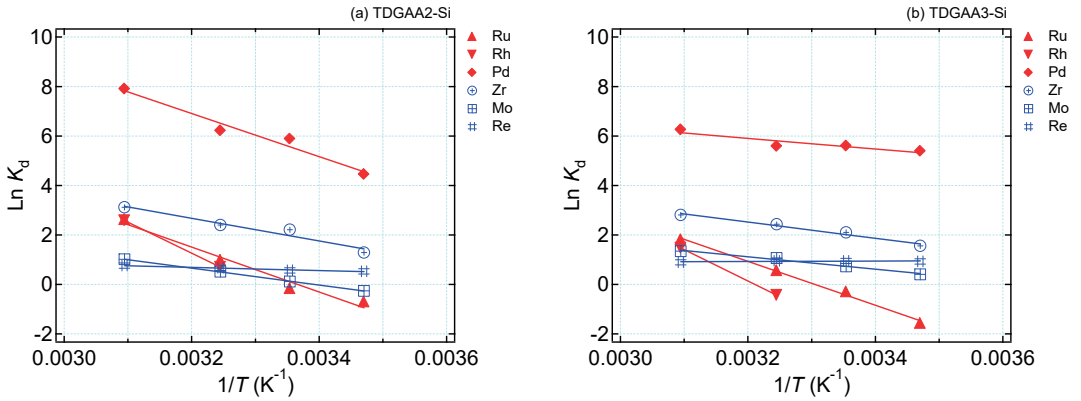

Figure 5. Effect of reaction temperature on the distribution coefficients of (a) TDGAA2-Si and (b) TDGAA3-Si. [Metal]: 5 mM for the 15 metal ions, [HNO_3]: 2 M, temperature: from 288 to 323 K, contact time: 5 h.

Table 1. Values of the thermodynamic parameters' values for the adsorption of Ru(III), Rh(III), Pd(II), Zr(IV), Mo(VI), and Re(VII) onto TDGAA2-Si and TDGAA3-Si.

	TDGAA2-Si						TDGAA3-Si					
	Ru(III)	Rh(III)	Pd(II)	Zr(IV)	Mo(VI)	Re(VII)	Ru(III)	Rh(III)	Pd(II)	Zr(IV)	Mo(VI)	Re(VII)
ΔG^0 (kJ mol^{-1})												
288 K	2.3	5.1	−10.9	−3.4	0.7	−1.2	3.6	8.0	−12.7	−3.9	−1.0	−2.3
298 K	−0.2	1.7	−13.8	−4.9	−0.3	−1.5	1.1	4.6	−13.8	−5.0	−1.8	−2.3
308 K	−2.8	−1.7	−16.7	−6.3	−1.3	−1.7	−1.3	1.2	−14.9	−6.1	−2.6	−2.4
323 K	−6.6	−6.9	−21.0	−8.5	−2.7	−2.0	−5.0	−3.9	−16.5	−7.7	−3.7	−2.5
ΔH^0 (kJ mol^{-1})	75.4	103.7	72.5	38.2	28.5	5.4	73.9	105.8	17.9	27.2	21.0	−0.9
ΔS^0 (kJ mol^{-1} K^{-1})	0.25	0.34	0.29	0.14	0.10	0.02	0.24	0.34	0.11	0.11	0.08	0.005

TDGAA3-Si, mean endothermic reaction, and the adsorption was enhanced by reaction temperature rise. While the tendency of adsorption of Ru(III) and Rh(III) corresponded with the results of some TDGA-type adsorbents [6-8], there was no significant difference in the adsorption temperature trends between TDGAA2-Si and TDGAA3-Si. In contrast, there was a slight difference in the sensitivity to Pd(II). The results regarding temperature dependence were well-fitted with those of the adsorption selectivity results shown in Figure 3. The negative ΔG^0 values indicated that Pd(II), Zr(IV), and Re(VII) adsorption onto TDGAA2-Si, and Pd(II), Zr(IV), Mo(VI), and Re(VII) adsorption onto TDGAA3-Si were spontaneous reactions at the experimental temperature conditions.

3.4. Adsorption and separation performances

The adsorption and separation behaviors of the 15 metal ions onto TDGAA-Si, TDGAA2-Si, and TDGAA3-Si at 298 and 323 K are shown in **Figure 6**. As shown in Figure 6, the uptake ratio R_C (%) of the metal ion is described as follows:

$$R_C = \frac{C_0 V_{Feed} - \int_0^{tVe} C_t V_f dt}{C_0 V_{Feed}} \times 100. \quad (5)$$

Table 2 summarizes the recovery ratios of Pd(II) and Zr(VI) from feed solution using TDGAA-Si, TDGAA2-Si and TDGAA3-Si. Investigations revealed that although all adsorbents completely absorbed Pd(II) at both temperature conditions, they were recovered by 0.1 M thiourea in 0.01 M HNO_3 eluent. Moreover, the Pd(II) eluent peak was sharp and could be recovered easily like the TDGA-type adsorbents [7,8]. Conversely, although Zr(IV) was well adsorbed onto TDGAA-Si at 298 K, it was almost unaccumulated on the adsorbent and partially drifted from the column in the presence of 2 M HNO_3. We also observed that the uptake ratio of Zr(IV) at an effluent volume (V_E) of 30 cm^3 showed a higher adsorption performance with TDGAA-Si than TDGAA2-Si and TDGAA3-Si due to the difference in reactivity with Zr(IV) when the contact time was short, e.g., within 10 min, the uptake ratio of Zr(IV) onto TDGAA-Si, TDGAA2-Si, and TDGAA3-Si in the batch-adsorption experiment was about 30% [9], 10%, and 10% (as shown in Figure 4), respectively. Furthermore, as shown by the experimental results on the adsorption selectivity and the effect of temperature, although the adsorption ratio of Ru(III), Rh(II), and Zr(IV) increased at 323 K, a similar tendency was not observed for Mo(VI) onto TDGAA-Si and TDGAA2-Si. The Zr(IV) peaks at 323 K and Re(VII) at 298 K with TDGAA3-Si, shifted farther than those of TDGAA-Si and TDGAA2-Si.

3.5. Effect of bed height

Depending on the bed height, adsorption and separation performances were evaluated using TDGAA3-Si, which had a significant peak shift of Re(VII). **Figure 7** shows the experimental results of varying the bed height h (80, 160, and 240 mm) at 298 K. Investigations revealed that the elution peak of Re(VII) was completely separated from the feed solution peak at a bed height of 160 mm, with most of its amount preserved. Conversely, although Zr(IV) and Mo(VI) were gradually adsorbed onto TDGAA3-Si, their peaks shifted. Based on these findings, we subsequently calculated the maximum peak positions for metal ions t_{metal}, e.g., t_{Re} for Re(VII), via the following equation:

$$t_{metal} = \frac{\int_0^\infty t C_t dt}{\int_0^\infty C_t dt}. \quad (6)$$

The difference between the adsorbed and nonadsorbed metal ion peaks, which correspond to the feed peak (t_{metal} - t_{Feed}), indicates the time for the adsorbed metal ion to react with the functional group of TDGAA3-Si. Specifically, $t_{metal} - t_{Feed}$ results indicate the order Re(VII) > Zr(IV) and Mo(VI) > Cs(I) and Ba(II), which favors the reaction with TDGAA3-Si, except for Pd(II) that was fully adsorbed onto TDGAA3-Si. TDGAA3-Si also has adsorption performance for Cs(I) and Ba(II), which were hardly adsorbed in the batch-adsorption experiments. Investigations revealed that the uptake ratio of Mo(VI), Ru(III), Ba(II), and part of Zr(IV) at an effluent volume of 60 cm^3 increased with the adsorbent's bed height, which was particularly effective for recovering Mo(VI) and Zr(VI) when TDGAA3-Si was used. Moreover, Re(VII) was almost not accumulated on the adsorbent while Re(VII) reactivity with TDGAA3-Si was high, as indicated by the peak shift. This observation may have resulted from the

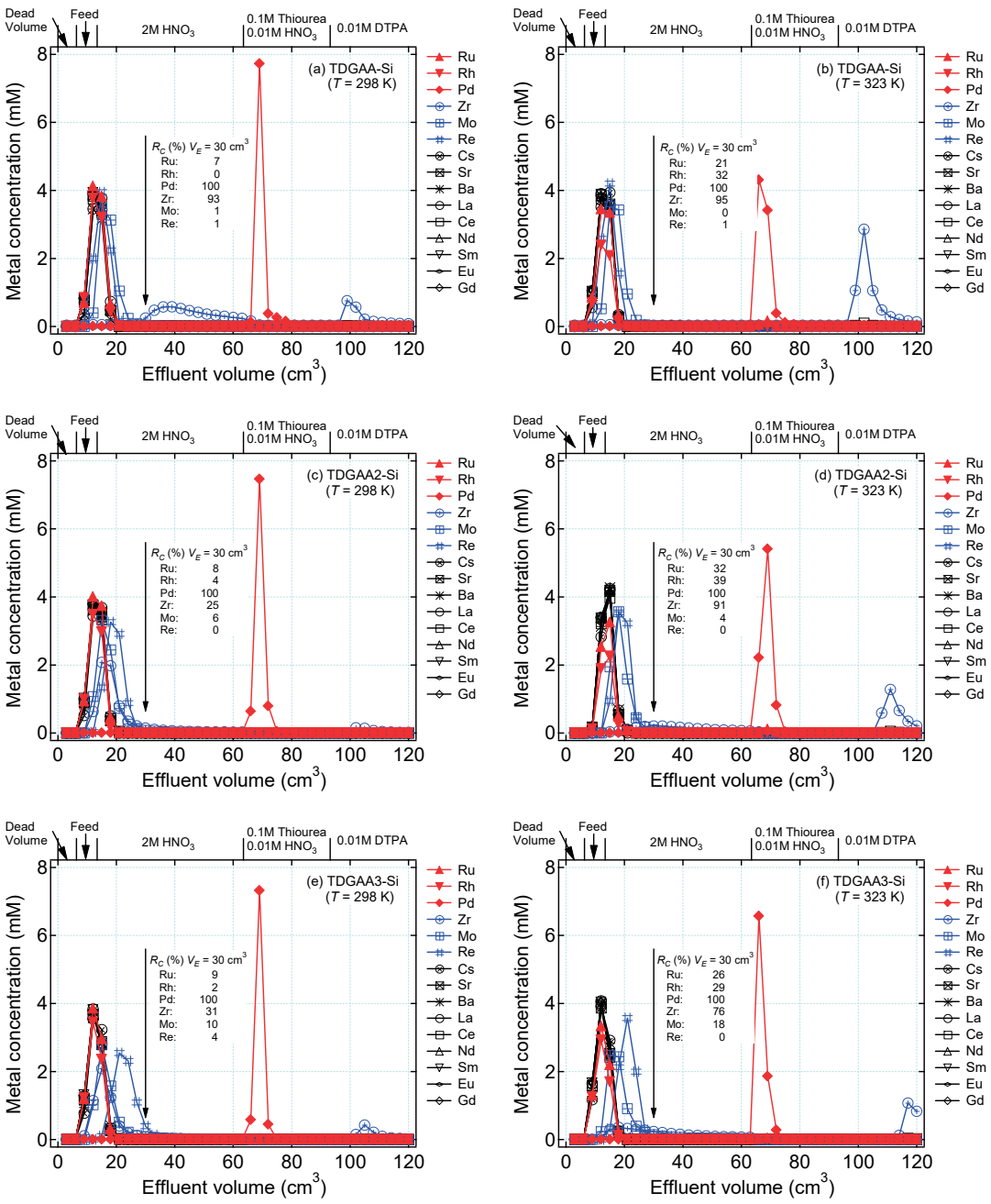

Figure 6. Chromatographic separation results for the 15 understudied metal ions, using (a, b) TDGAA-Si, (c, d) TDGAA2-Si, and (e, f) TDGAA3-Si. [Flow rate: 0.3 cm^3 min^{-1}, bed height: 80 mm, inner diameter of the column: 10 mm, and temperature: 298 and 323 K] (DTPA: diethylenetriamine pentaacetate acid).

Table 2. Recovery ratios of Pd(II) and Zr(IV) from feed solution using TDGAA-Si, TDGAA2-Si, and TDGAA3-Si.

Recovery ratio (%)	TDGAA-Si		TDGAA2-Si		TDGAA3-Si	
	Pd(II)	Zr(IV)	Pd(II)	Zr(IV)	Pd(II)	Zr(IV)
298 K	97	84	97	12	98	15
323 K	93	82	94	54	98	40

presence of Re(VII) in the nitric acid solution in the form of perrenate ion (ReO_4^-), which competes with nitric acid ion during the adsorption process [15-17].

4. Conclusion

Herein, to reduce the volume of high-level radioactive waste and to obtain scarce resources by separating metal ions from HLLW, three types of thiodiglycolamic acid-

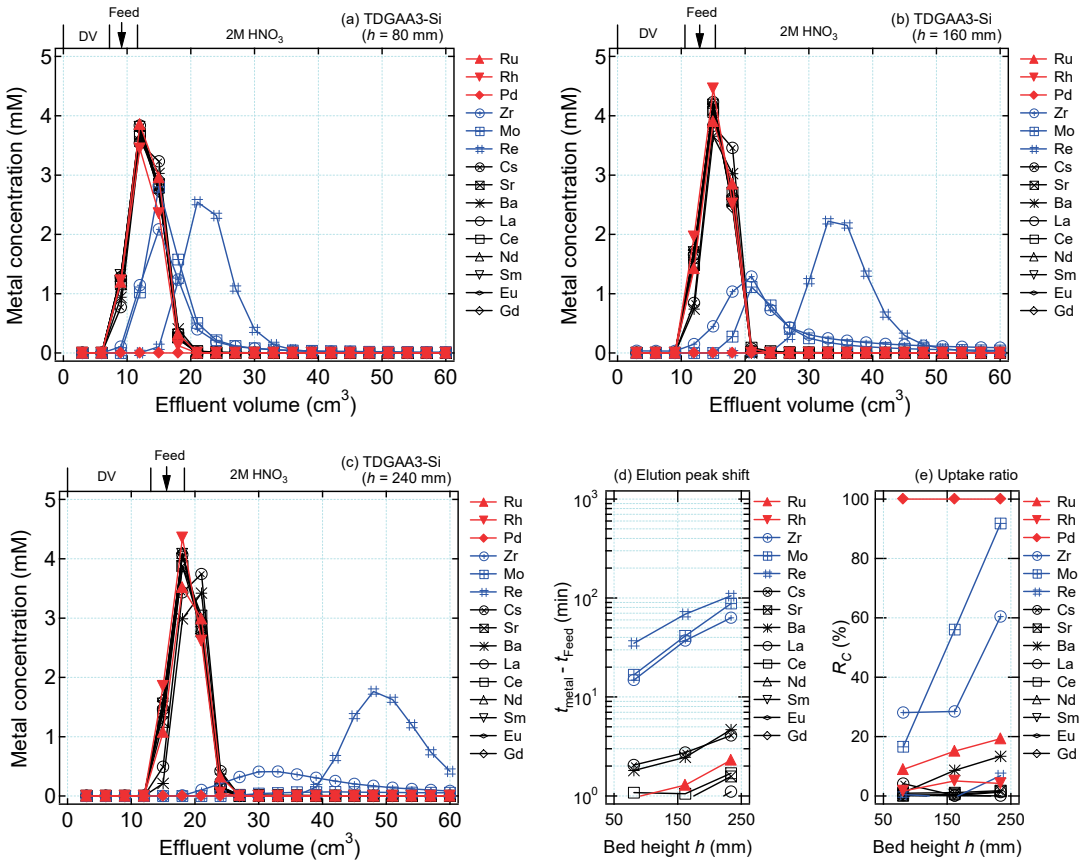

Figure 7. The (a–c) chromatographic separation results, (d) elution peak shift, and (e) uptake ratio at an effluent volume of 60 cm^3 for the 15 metal ions, using the TDGAA3-Si varying bed height. [Flow rate: 0.3 cm^3 min^{-1}, bed height: 80, 160, and 240 mm, inner diameter of column: 10 mm, and temperature: 298 K].

functionalized silica gel: TDGAA-Si, TDGAA2-Si, and TDGAA3-Si, were synthesized using thiodiglycolic anhydride and three functionalized silica gels: 3-aminopropyl-functionalized silica gel, 3-(ethylenediamino)propyl-functionalized silica gel, and 3-(diethylenetriamino)propyl-functionalized silica gel. From the batch-adsorption experiments, although the basic adsorption performances of TDGAA2-Si and TDGAA3-Si were almost similar, adsorption performance differences existed due to their partly different structures. For instance, while TDGAA2-Si showed a high uptake ratio of Ru(III), Rh(III), and Zr(IV) than TDGAA3-Si when the adsorption time was increased, the temperature sensitivity of adsorption of Pd(II) was confirmed when TDGAA2-Si was used. Both adsorbents improved the adsorption performances of Ru(III), Rh(III), Pd(II), Zr(IV), and Mo(VI) at elevated temperatures. As observed in chromatographic separation experiments, while Pd(II) was completely recovered from the feed solution using the three adsorbents and 0.1 M thiourea in 0.01 M HNO_3 as eluent, Ru(III) and Rh(III) were difficult to separate at 298 K. However, their uptake ratio could be improved by raising the temperature as indicated by the batch-adsorption experiments. Investigations also revealed that only TDGAA-Si showed a high uptake Zr(IV) ratio, even when the temperature was 298 K. The peak of Zr(IV) and Re(VII) was retarded using TDGAA3-Si. Overall, as a result of evaluating the adsorption properties of TDGAA3-Si using the column based on bed height changes, we confirm that while Zr(IV) and Mo(VI) are most suitable for accumulation on the adsorbent, Re(VII) is suitable for separation via peak shifts by setting an appropriate bed height. These results demonstrate the potential for separating and recovering Pd(II), which is a scarce resource, while reducing the volume of high-level radioactive waste by isolating individual metal ions from HLLW.

References

[1] IAEA (1997), Techniques for the solidification of high-level waste, *IAEA Technical Reports Series* 176.

[2] L. Rodriguez-Penalonga and S.Y. Moratilla, A review of the nuclear fuel cycle strategies and the spent nuclear fuel management technologies, *Energies* 10 (2017), p. 1235.

[3] K. Zdenek and R.V. Edouard, Recovery of value fission platinoids from spent nuclear fuel part I: general considerations and basic chemistry, *Platinum Metals Review* 47 (2003), pp. 74-87.

[4] A. Zhang, Y. Wei, M. Kumagai and Y. Koma, A new partitioning process for high-level liquid waste by extraction chromatography using silica-substrate chelating agent impregnated adsorbents, *Journal of*

Alloys and Compounds 390 (2005), pp. 275-281.
[5] A. Zhang and Q. Hu, Adsorption of cesium and some typical coexistent elements onto a modified macroporous silica-based supramolecular recognition material, *Chemical Engineering Journal* 159 (2010), pp. 58-66.
[6] Y Xu, S-Y. Kim, T. Ito, T. Tada, K. Hitomi and K. Ishii, Adsorption properties and behavior of the platinum group metals onto a silica-based (Crea + TOA)/SiO_2-P adsorbent from simulated high level liquid waste of PUREX reprocessing, *Journal of Radioanalytical and Nuclear Chemistry* 297 (2013), pp. 41-48.
[7] H. Wu, S-Y. Kim, M. Miwa and S. Matsuyama, Synergistic adsorption behavior of a silica-based adsorbent toward palladium, molybdenum, and zirconium from simulated high-level liquid waste, *Journal of Hazardous Materials* 411 (2021), 125136.
[8] N. Osawa, M. Kubota, H. Wu and S-Y. Kim, Development of *N*,*N*,*N*′,*N*′-tetra-2-ethylhexyl-thiiodiglycolamide silica-based adsorbent to separate useful metals from simulated high-level liquid waste, *Journal of Chromatography A* 1678 (2022), 463353.
[9] T. Ito and S-Y. Kim, Study on separation of platinum group metals from high-level liquid waste using sulfur-containing amic acid-functionalized silica, *Journal of Ion Exchange*, 29 (2018), pp. 97-103.
[10] N. Osawa, T. Ito, H. Wu and S-Y. Kim, Study of the applicability of a functionalized silica-based adsorbent for Pd(II) separation from simulated high-level liquid waste, *Journal of Ion Exchange* 33 (2022), 127-134.
[11] T. Ogata, H. Narita and M. Tanaka, Adsorption mechanism of rare earth elements by adsorbents with diglycolamic acid ligands, *Hydrometallurgy* 163 (2016), pp. 156-160.
[12] R.G. Pearson, Hard and soft acids and bases, *Journal of the American Chemical Society* 85 (1963), pp. 3533-3539.
[13] M. Naushad, Z.A. ALOthman, Md. Rabiul Awual, MM. Alam and G.E. Eldesoky, Adsorption kinetics, isotherms, and thermodynamic studies for the adsorption of Pb^{2+} and Hg^{2+} metal ions from aqueous medium using Ti(IV) iodovanadate cation exchanger, *Ionics* 21 (2015), pp. 2237-2245.
[14] E.C. Lima, H-B. Ahmad, M-P. Juan Carlos, I. Anastopoulos, A critical review of the estimation of the thermodynamic parameters on adsorption equilibria. Wrong use of equilibrium constant in the van 't Hoff equation for calculation of thermodynamic parameters of adsorption, *Journal of Molecular Liquids* 273 (2019), pp. 425-434.
[15] F. Ichikawa, S. Uruno and H. Imai, Distribution of various elements between nitric acid and anion exchange resin, *Bulletin of the Chemical Society of Japan* 34 (1961), pp. 952-955.
[16] K. Shimojo, H. Suzuki, K. Yokoyama, T. Yaita and A. Ikeda-Ohno, Solvent extraction of technetium(VII) and rhenium(VII) using a hexaoctylnitrilotriacetamide extractant, *Analytical Sciences* 36 (2020), pp. 1435-1437.
[17] N. Osawa, S-Y. Kim, T. Ito and H. Wu, Effect of adding dodecanol as modifier to *N*,*N*,*N*′,*N*′-tetra-*n*-hexyl-3,6-dithiaoctane-1,8-diamide silica-based adsorbent on the adsorption behaviors of platinum-group metals and other metals from simulated high-level liquid waste, *Radiochimica Acta* 109 (2021), pp.867-876.